

# THE CORRESPONDENCE PROBLEM IN THE OPTICAL SHAPE AND DEFORMATION MEASUREMENT METHODS

Stjepan Jecić, Nenad Drvar

## Summary

How to correctly locate and uniquely index the same image point during the optical measurements is known as the correspondence problem. It occurs when there is a need for tracking features in all of the recorded images, regardless of the number of used cameras and the number of recorded images. In this paper, we have compared the correspondence problem solutions for the passive and active single, stereo and multi-camera systems, with a special focus to the active multi-camera system, for which we present the absolute method for unique stereo pair indexing. By using a modified projection approach, we have showed that it is possible to eliminate the need for the epipolar principle from the correspondence problem solving. With the new indexing method, each pixel can be used as a separate measuring point since it has been indexed with two independent absolute phases. Searching for stereo pairs has also been reduced from the two-dimensional image domain to a one-dimensional array, where the next stereo pair is most likely the nearest neighbor to the observed one.

*Keywords:* optical measurement, shape, deformation, multi camera systems, correspondence problem, phase shifting, Gray code, digital image correlation

## 1. INTRODUCTION

Optical discrete and full-field deformation measuring methods are quickly gaining importance because of their speed and the amount of data that can be gathered compared to contact measurement methods. The benefits of optical applications have been recognized in various industrial and scientific fields, such as: medicine [1]; material research; automotive; shipbuilding [2] and aerospace industries; transportation; power generation; design; heritage preservation and civil engineering. In this paper, methods of solving the correspondence problems that exist in the optical methods suitable for deformation and shape measure-

ments will be critically evaluated for passive and active single and multi camera systems. A special focus will be set on the stereo and multi-camera systems where contribution to the correspondence problem solving is presented. Problem of locating and uniquely indexing the same image point (or feature) in all images exists in the optical measurement methods and is known as the correspondence problem. The correspondence problem occurs when there is a need for tracking features in all of the recorded images, regardless of the number of used cameras and the number of recorded images. Image features carry important displacement or shape information, thus their number per image tends to be large. The correspondence problem also exists in the human vision system, where two eyes are equivalent to two cameras in vision systems. The brain is able to find stereo pairs and reconstruct 3D scene even in the occurrence of noise, seemingly in real time, without our awareness and our conscious involvement in the process. It relies on the existence of logical structures in the viewed scene, but it can also be proven that they are not needed by the existence of random dot stereograms. One of the reasons for the existence of the correspondence problems in computer vision is that computers cannot comprehend image (and the space it represents) in the same way human vision can. In order to enable computers to solve the correspondence problem, it is necessary to prepare the scene in such a way that recorded pixel matrix contains structure that is uniquely recognizable in all the recorded images. It is also necessary to develop suitable algorithms, which can uniquely identify as many stereo pairs as possible in all of the recorded images. Regarding the way current methods define the measurement point, they can be considered passive and active. Passive methods for stereopair recognition use regular or random optical patterns which need to be firmly attached to the surface of the measuring object. Various markers can be used, e.g. circular coded and non-coded stickers or crosses, random pattern obtained by spraying with the contrast paint or natural surface pattern like on marble surfaces. Active methods use some sort of the projected monochromatic coherent laser beam or non-coherent white light, which can further be subdivided in time-dependent, object and direct methods. The systems based on passive methods define measuring point as a group of pixels, while active systems can in some cases even index each pixel separately, which enables the digitization of discontinuities and complicated object surfaces.

## 2. SINGLE CAMERA DEFORMATION MEASUREMENT

Single camera systems are nowadays used for deformation measurements as video extensometers for automated measurements of material mechanical pro-

perties. Optical markers can be defined as a large variety of shapes, for example: lines, crosses, coded and non-coded dots, random pattern or speckles caused by laser illumination, Figure 1.

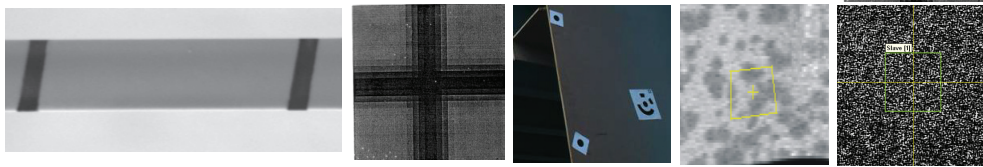


**Fig. 1** Optical marker samples

**Sl. 1.** Primjeri optičkih markera

The camera is usually placed perpendicular to the specimen surface which can be either flat or round (Figure 3), and uses 2D image plane to record the position of markers in 3D space (Figure 2). This process can be described by perspective mapping and results in a partial information loss. In order to conduct the deformation measurements on the image plane, one has to insure that specimen deformation only occurs parallel to the image plane. Some laser extensometer systems use two cameras (e.g. LSE produced by Messphysik). The deformation is measured by observing the displacements of speckles in the zone where laser-projected dots light the specimen surface. The diameter of LSE's laser dots is 2-4 mm, but the area of interest can be in the range of  $1/10 \text{ mm}^2$ . Because of the required magnification, each camera can see only one of the markers and the camera exterior orientation parameters are not known; the triangulation of spatial points is not possible. The knowledge of the scene allows the usage of the vanishing point principle together with homography to reconstruct 3D data from a single image. That information is not suitable for accurate shape measurement purposes; it is only suitable for visualization purposes. If the deformation of some object is considered pseudo static, it is possible to measure it by recording each of the loading stages individually by a single camera system (Section 2.2.). For triangulation to take place, the camera needs to record the object from different positions in the surrounding space. Such system needs to be able to reconstruct the camera internal and external parameters and to triangulate position of spatial markers in space. It has to be based on the bundle adjustment principle for solving the equations of projective mapping; such systems are nowadays commercially available (e.g. Tritop by GOM).

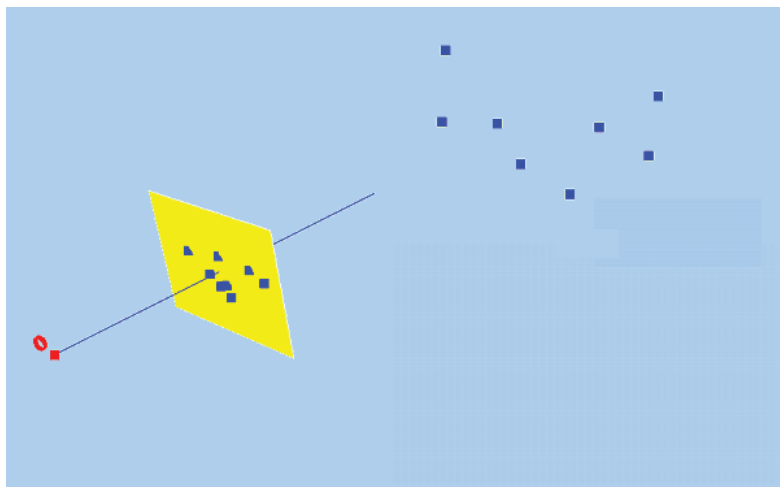


*Fig. 2* Mapping 3D information to 2D image plane

*Sl. 2.* Preslikavanje iz 3D prostora u 2D ravninu slike

## 2.1. Video extensometers

Let us begin with examining how a mechanical strain gauge measures displacements between two points on the specimen to which it is firmly attached. If the effect of the friction between specimen and grips can be neglected, together with errors in the necessary electric measurements, the measuring points are believed to correspond with the position of contacts between specimen and grips. For the uniaxial measurements of the material properties, strain gauge with two grips is sufficient if we focus on the deformation that follows the specimen's largest axis. Measured strains are an integration of local strains, since this method cannot take into account the local effects of necking. Mechanical extensometer can be replaced by a fixed single camera setup [3], also known as the video extensometer (Figure 3) which tracks markers attached to the specimen surface (there are dual camera versions that project markers with laser, e.g. LSE produced by Messphysik). In order to mimic the same experiment with the optical non-contact methods, measurement points need to be defined in the same position on the specimen surface as for the mechanical strain gauge. If flat specimen is used, the correspondence problem that needs to be solved is how to track the same measurement points in multiple sequential images. For the system shown in Figure 3, measurement points are defined by a cross-section of lines defining each linear marker and a line defining the specimen's longest axis. Since there are no mechanical parts, more information can be gathered simply by adding more than two optical markers,

which further complicates the correspondence problem but gives more information for the same number of images.

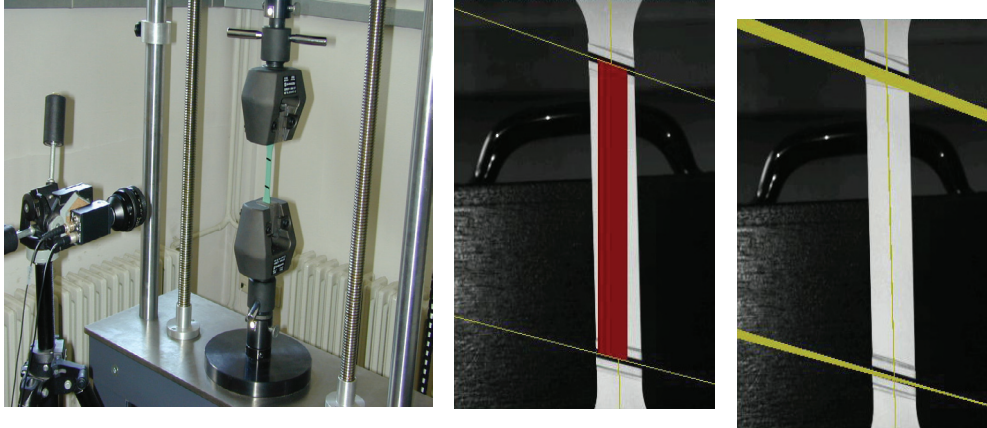


**Fig. 3** Single camera measurement setup (left), displacement visualization (right)

**Sl. 3.** Mjerna postava jedne kamere (lijevo), vizualizacija pomaka (desno)

For a system with two linear markers (Figure 3) in the first stage, each marker has to be localized (by using either threshold or knowledge of the scene – light specimen surrounded by dark background to the sides and dark markers on top and bottom). Marker localization can be conducted by locating border [4], or the center of gravity of the area. For both methods, border should have a good contrast relative to the specimen surface. Borders can be located by using thresholds or edge image filtering, Figure 4.

Defining threshold value depends on the marker definition, camera settings and marker orientation with regard to rows of camera pixels [3]. Figure 4 shows graphs for two characteristic cross sections: 1 is for the edge of the specimen needed for finding the longest axis; 2 is for the marker. The line profile brings light intensity across sections, while bar plots show light intensity of the gradient filtered results. Threshold location should be placed on the point of inflection between specimen and marker or background, but due to the discrete nature of pixels, that point is not always clearly visible in the line profile. The edge filter has the biggest response in the point of the largest gradient, thus helping the threshold location. For a given profile location of the center of gravity of the area between threshold and intensity profile line is shown in Figure 5. In the 8-bit camera and the ideal object-marker setup, the ideal threshold would be at the half of the measurement range, or 128. Should we choose 100 or 120, from the simulation in

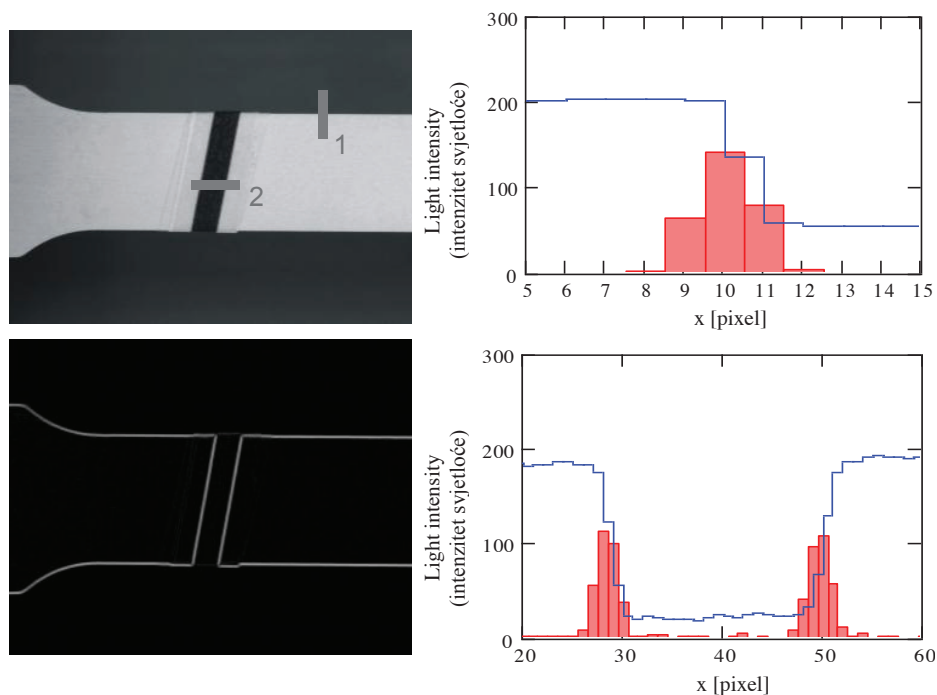


**Fig. 4** Marker feature localization by thresholding (upper left); gradient filtering (lower left); intensity profiles for section 1 (upper right) and section 2 (lower right)

**Sl. 4.** Određivanje položaja markera preko gradijenta (lijevo gore), gradijentnim filtriranjem (lijevo dolje), profil svjetloće za presjek 1 (desno gore) i presjek 2 (desno dolje)

Figure 5 it is visible that the location of the center of gravity will differ in less than 0.03 pixel, meaning that operator has decent sub-pixel accuracy. After each marker is successfully localized in the current stage, its location has to be found in the next stage image. This is helped by the knowledge of the expected displacement; its position can be found in an area defined by e.g. 5% of the current location, which speeds up the analysis since the operator need not search the entire image looking for marker. Since there are only two markers involved and loading conditions are known, their IDs are not expected to change places; thus no additional numbering is required. Figure 3 illustrates reference (unloaded stage) and one of the loading stages, for the visualization purposes lines are leaving a trail of marker position in time. The lower marker has fewer displacements than the upper marker, which was near the moving crosshead. There is a small inclination between the specimen axis and the displacement of the machine, which is visible as the slightly non-parallel marker line positions in time.

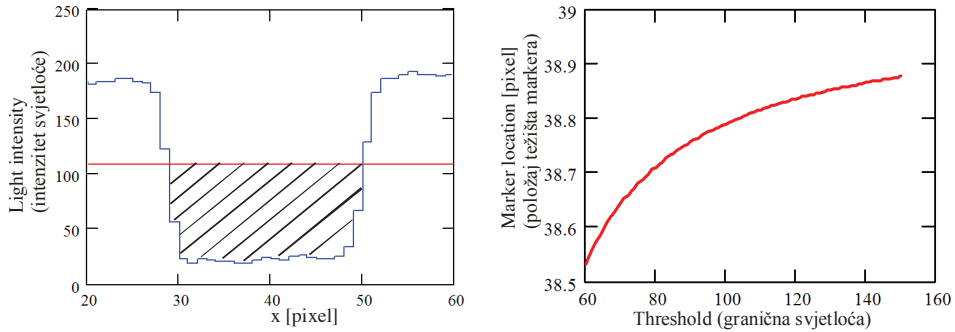


**Fig. 5** Marker location by the center of gravity measurement

**Sl. 5.** Određivanje položaja markera preko mjerenja položaja težišta

If testing machine needs to be strain controlled, then chosen optical measurement method has to feed real-time strain data back to the machine, rendering the correspondence problem solving a time critical process.

## 2.2. 3D measurements with a single camera

If each optical marker is visible only in one camera (Figures 2, 3) the spatial coordinates of measuring points cannot be measured, since 3D space is perspective mapped onto a 2D image plane. In turn, all strains can be measured only on the image plane, thus any deviation from the planar displacements of the observed specimen surface cannot be detected, and together with lens aberrations, it will most likely be the cause of systematic measurement errors, which motivates the development of stereo systems based on a single camera, Figure 6 (left).

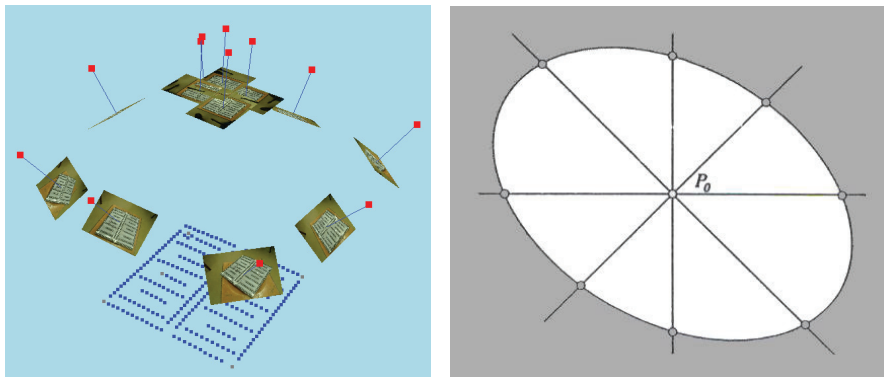


**Fig. 6** Single camera shape measurement (left), circular marker localization (right)

**Sl. 6.** Mjerenje oblika s jednom kamerom (left), težište kružnog markera (desno)

By using the perspective projection, it is possible to mathematically map spatial coordinates to the image (Figure 8), providing that camera internal and external orientation parameters are known. Internal camera parameters depend on the optical components used; hence it is possible to make them constant in time by fixing the lens focus and aperture parameters. External parameters define the camera position and orientation in time (the left side of Figure 6 shows an object recorded by single camera from multiple locations), and they can be calculated by bundle adjustment provided that markers on the object are stable in time and marked in a way that explicitly enables unique marker identification. For this purpose, circular markers are more suitable than linear ones. They can be coded by color, size or additional rings around them. All non-coded markers usually have the same visual characteristics; thus their identification codes have to be uniquely assigned by exploiting their unique position in space. Marker location in each image can be found by threshold and localization algorithms, followed by the localization of each marker's center of gravity. This is done by locating points on the edge and fitting ellipse through the edge (Figure 6 right). For pseudo static deformation measurements, it is sufficient to measure marker locations in each loading stage and calculate relative displacements for points with the same identifier, Figure 7.

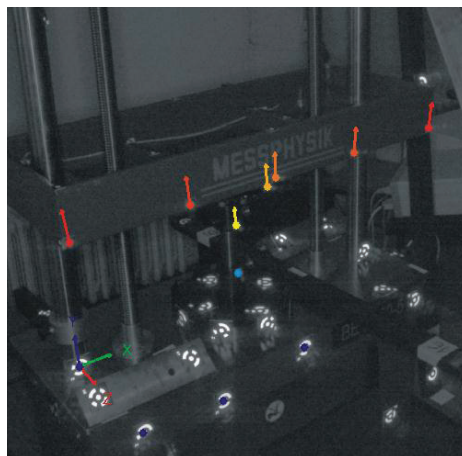
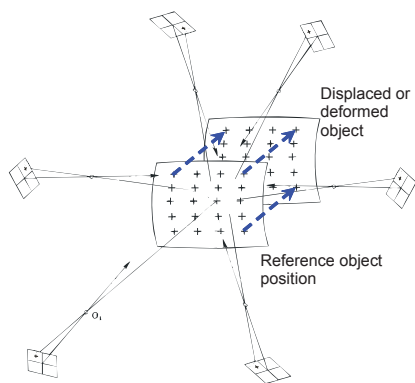


**Fig. 7** Single camera displacement measurement

**Sl. 7.** Mjerenje pomaka s jednom kamerom

The bundle adjustment principle will be explained on a model of ideal pinhole camera [5-7], without parameters that describe the lens aberration influences which can be later added to the model as nonlinear factors. Based on a collinea-

rity of the lens center point  $O$  and the spatial object coordinate of a point  $P$  (Figure 8), image coordinates can be related to spatial object coordinates:

$$\begin{bmatrix} X \\ Y \\ Z \end{bmatrix}_i = \lambda_{ij} \mathbf{R}_j \begin{bmatrix} x_{ij} - x_{0j} \\ y_{ij} - y_{0j} \\ 0 - c_j \end{bmatrix} + \begin{bmatrix} X_0 \\ Y_0 \\ Z_0 \end{bmatrix}_j \quad (1)$$

While index  $i$  relates to the numerical index of the observed spatial point, and index  $j$  to the camera used (or image number if all the images are recorded by a single camera from multiple orientations),  $\mathbf{R}_j$  is the orthogonal rotation matrix between image and object coordinate systems. If we dismember Eq. (1) so that left of the equation sign are image coordinates, and scale factor of the imaging ray  $\lambda_{ij}$  omitted by cancelling out, the relation between image and object coordinates is given by:

$$x_{ij} = -c_j \frac{r_{11j}(X_i - X_{0j}) + r_{21j}(Y_i - Y_{0j}) + r_{31j}(Z_i - Z_{0j})}{r_{13j}(X_i - X_{0j}) + r_{23j}(Y_i - Y_{0j}) + r_{33j}(Z_i - Z_{0j})} + x_{0j} \quad (2)$$

$$y_{ij} = -c_j \frac{r_{12j}(X_i - X_{0j}) + r_{22j}(Y_i - Y_{0j}) + r_{32j}(Z_i - Z_{0j})}{r_{13j}(X_i - X_{0j}) + r_{23j}(Y_i - Y_{0j}) + r_{33j}(Z_i - Z_{0j})} + y_{0j} \quad (3)$$

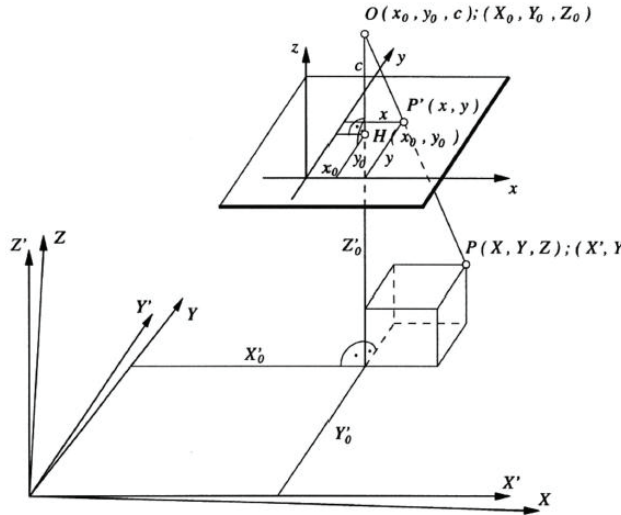


**Fig. 8** Camera projection model  
**Sl. 8.** Projekcijski model kamere

The bundle adjustment model can be applied to general photogrammetric problems that can be defined as the following setups:

- a general problem in which all parameters on the right side in equations 2 and 3 are unknown,
- the determination of external calibration parameters, if internal are known (e.g., the orientation of metric cameras);
- the internal orientation and coordinates of object points are known, the external orientation parameters are computed;
- only the coordinates of object points are known; it is necessary to determine the parameters of internal and external orientation;
- parameters of internal and external orientation are known; the coordinates of object points can be calculated.

### 3. STEREO CAMERA SYSTEMS

By using more than one camera (Figure 9), optical systems become over determined, which enables the measurement of the actual spatial coordinates for the observed markers. Here the previous correspondence problem definition has to be extended in order to take into account the need for locating the observed point stereo pairs in the additional cameras.

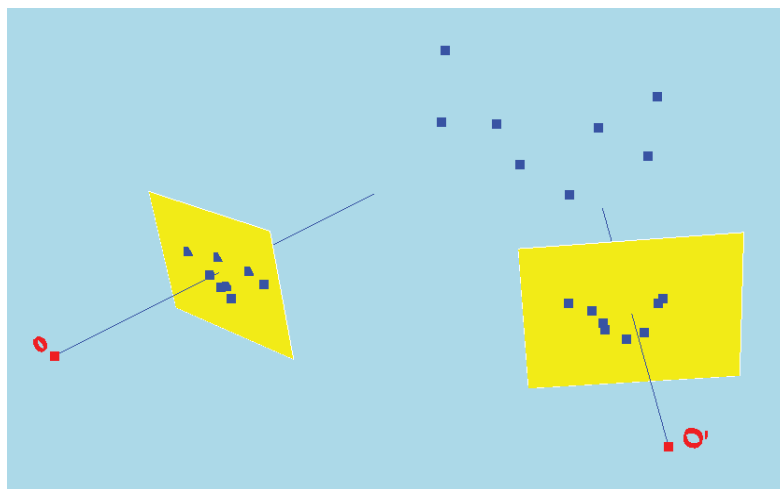


**Fig. 9** Mapping 3D information to two camera image planes

**Sl. 9.** Preslikavanje prostornih koordinata u dvije ravnine slike

Should more than one deformation stage be observed, the correspondence problem will also depend on time. This happens because different loading sta-

ges need to be mutually compared for the strain calculation to take place. If the importance of time between each measurement stage is neglected, each deformation stage becomes a 3D point cloud describing the model's current shape. This means that the correspondence problems are actually similar in both the shape and deformation measurements. Optical markers can consist of a single pixel or a group of pixels (Figure 1). The specimen surface can be monochromatic, reflective, transparent, colored, as well as planar, curved or containing various artifacts that can distort or damage marker projection to the additional cameras [8, 9]. In order to solve the correspondence problem each characteristic marker should appear in each image only once (Figure 9). This condition is not straightforward to satisfy (Figure 10), because cameras have limited light intensity resolution depths together with the ability to simultaneously measure a large number of measurement points, nowadays in the mega pixel range. It can also be influenced by the surface characteristics that can cause apparent object point repeatability (e.g. repeatable surface features such as threads in cloths) or can be caused by the usage of non coded circular stickers or regular drawn mesh (Figure 10).

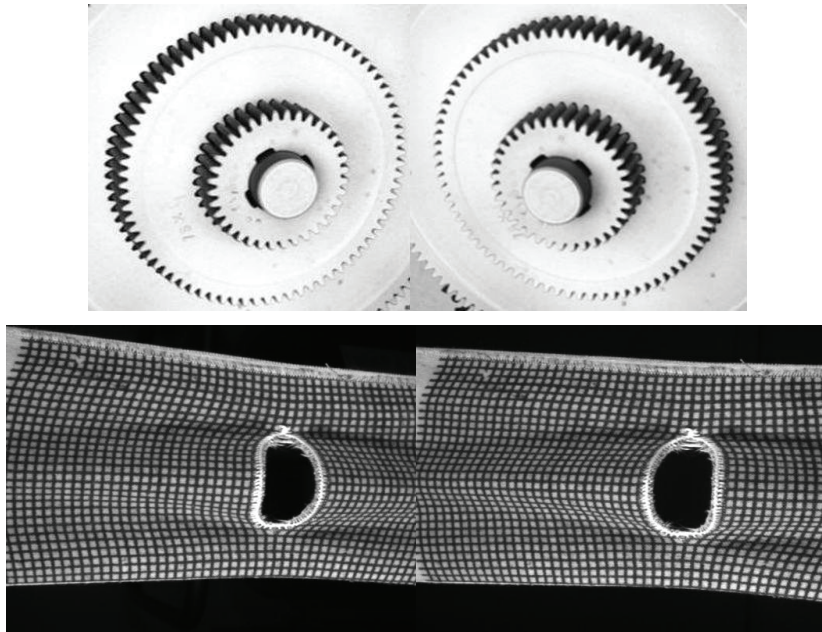


**Fig. 10** Stereo image specimen samples prepared for digitization with: active system (upper pair); passive system (lower pair)

**Sl. 10.** Primjeri stereo slika uzorka pripremljenog za digitalizaciju: aktivnim sustavom (gornji par), pasivnim sustavom (donji par)

In order to record a single stage with two cameras they have to be oriented in such a way that the recorded images overlap (Figure 11). In the case with two parallel cameras, the overlapping increases as cameras are brought closer. In that case, triangulation accuracy decreases, since the base distance between cameras becomes much smaller than the distance to the object surface. By increasing the base distance, the accuracy improves and the overlapping decreases, thus requiring additional measurements to cover the entire surface of the measurement object. The surface artifacts can also cause occlusions when parts of the surface are visible either in only one or in no camera, leading to the loss of data or to errors in measurements (Figure 11).

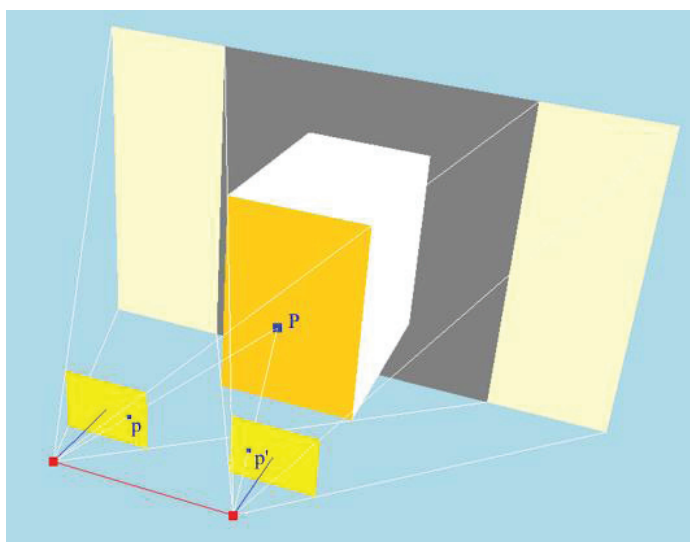


**Fig. 11** Parallel camera overlap visualization

**Sl. 11.** Vizualizacija preklopa kod sustava paralelnih kamera

The motivation for the correspondence problem solving in stereo systems is to enable the system calibration, as well as the point cloud triangulation on the complete measurement object surface. Should a model consist of only one object point (Figure 11), the correspondence problem would not exist, because in each recorded image, a single location belonging to the image of this marker would exist (e.g. single-point laser projection).

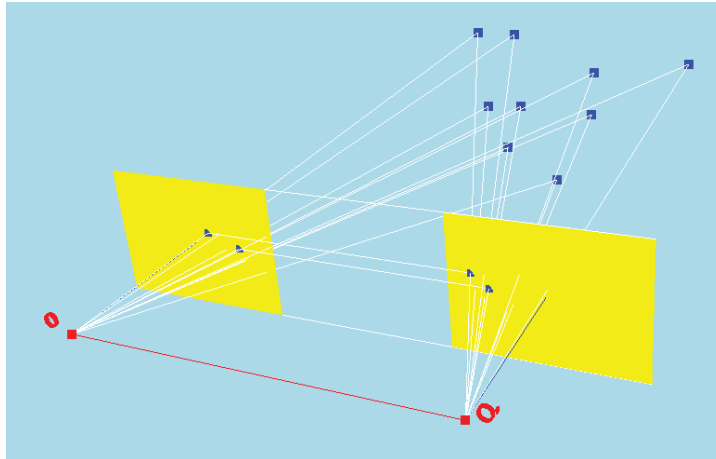


**Fig 12** Visualization of the correspondence problem for parallel stereo camera setup

**Sl. 12.** Vizualizacija problema jednoznačnosti kod sustava s dvije paralelne kamere

The illustration of the correspondence problems for stereo systems will be conducted on a non-calibrated passive stereo camera system consisting of two identical parallel cameras. Instead of the image of a real measurement object, here it is practical to use discrete point cloud. If the correspondence problem were a priori solved, lines passing through blue points (spatial point locations) and red points (camera projection centers) would pass through their image points in the respective image plane. For two stereo pairs, this is illustrated in Figure 12. If spatial coordinates of the measurement points and the position and orientation of cameras in space were known, the correspondence problem would be automatically solved because image markers would have to be on a line connecting spatial point with the camera projection center  $O$ . For stereo systems, the location and orientation of the camera system and spatial coordinates are usually not a priori known. Let us further simplify this model by neglecting the lens influence on the path on which the light beams travel from the object surface to the image plane. Cameras are here visualized by using the image plane in the virtual positive projection; that way image is not inverted. Parallel setup is chosen because it introduces significant simplifications to the model. If the second camera is obtained by the replication and translation of the first camera, then searching for stereo pairs in two images is simplified from full 2D image search to search along the single line. In parallel setup, horizontal pixel rows remained horizontal during the second camera ideal translation. Epipolar lines are thus horizontal and

mutually parallel for different object points (or sometimes even collinear). The stereo pair with features most similar to the chosen image point in the reference image can be found along the same horizontal line of pixels in the second camera. When the stereo pair is found, its relative position in the second camera can be easily visualized as disparity image, where each pixel represents a distance in the horizontal direction of stereo pairs in both images. Let us further simplify this model so that the observed scene consists of only three identical object points, as seen in Figure 13. Object points are colored differently (blue, red and green) just for the visualization purposes; we will assume that cameras see them as if their color, intensity and size is the same for all points. The correspondence problem here is how to recognize which image points belong to the stereo pair of the point  $P$  in the left camera and the right camera.

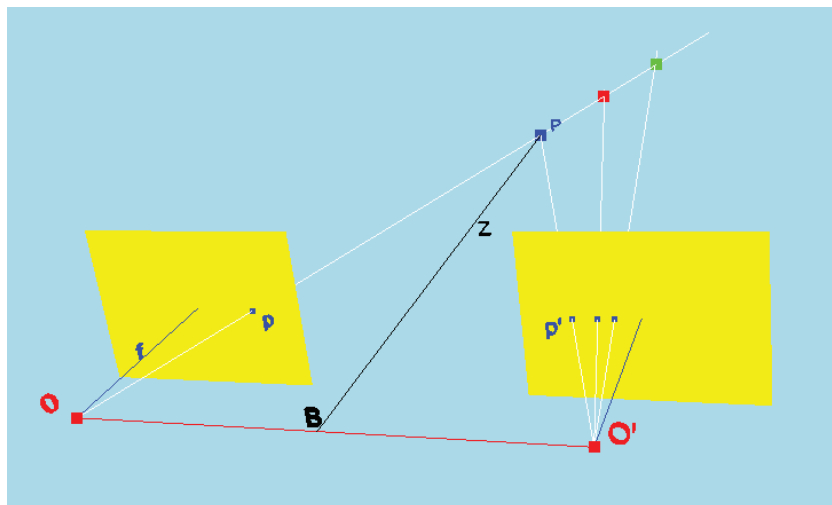


**Fig. 13** Simplified correspondence problem model with three stereo pairs

**Sl. 13.** Pojednostavnjeni model problema jednoznačnosti sa tri stereo para

For a given camera setup, spatial points are chosen in such a way that in the left camera all three points are visible as a single image point  $p$ , while in the right camera all three spatial points will have their image points. Because of the chosen parallel setup, it is clear that all three points in the right camera must lie in the same horizontal pixel row as the image point  $p$  in the left image plane. As a consequence of this object point distribution, the correspondence problem in the left camera is automatically simplified since there is only one image point recorded. In order to completely solve the correspondence problem for point  $P$ , in the next

step it is necessary to eliminate the excessive image points in the right camera. By observing Figure 13, it becomes clear that for the chosen spatial point configuration, the order of spatial points coincides with the order of image points, thus the first stereo pair can be only the first image point from the left side, marked as  $p'$ . The order of spatial points is not always usable since it is possible that some image points are not always visible in both cameras, or that the order of points is not the same, because they are placed on different distances from the baseline. Given a large number of points that can be recorded by modern cameras (and scenes are mostly unknown), it is not always possible to help solving the correspondence problem by using the distribution of object points. The consequences of the erroneous stereo pair recognition are clearly visible if we falsely conclude that the wanted  $p'$  in the right camera is the second or the third image point. In that case, the triangulated spatial location of the point  $P$  would belong to the red or green point, which can drastically deviate from the actual point  $P$  location. In this example, except for the assumption of the order of image points, there are no other mechanisms to detect erroneous stereo pairs. In case of non-parallel cameras, the above assumption regarding the horizontal stereo pair position in the right image is no longer valid, and stereo pairs could lie anywhere in the 2D image domain. It is known that this problem can be overcome by the reconstruction of the epipolar line, along which the wanted stereo pair should lay. One has to calculate the fundamental matrix  $F$  and eventually conduct the rectification procedure. In previous examples, we used a discrete point cloud with the assumption that we can locate and mutually differentiate each image point in each of the recorded images.

### 3.1. Homography

The known system and object geometry can be utilized for accurate or approximate stereo pair locating. They are not always known, e.g. the system is not yet calibrated or nothing is known about the object to be measured. Plane homographies [10] are projection transformations that can describe how points project from plane to plane.

$$p' = Hp \tag{4}$$

Equation 4 describes how point  $P$  projects from the plane in object space to point  $p$  in the image plane, or in this case its projection from one image plane to the other ( $p \Leftrightarrow p'$ ), Figure 14. For each point it is necessary to know the homography matrix  $H$ , which can be determined [11] under the condition that the observed object is locally planar, and at least 4 stereo pairs are known for the ob-

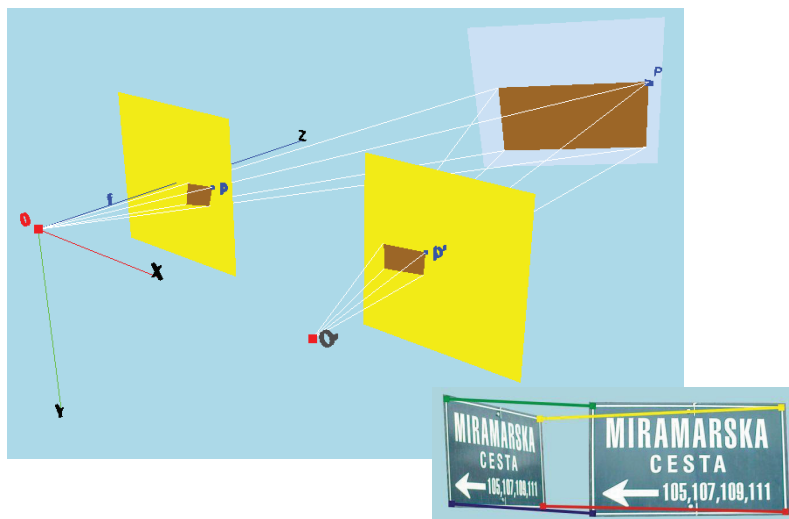


**Fig. 14** Plane homography camera relations

**Sl. 14.** Veza kamera preko ravninske homografije

served plane (Figure 14, lower right corner). Point to point transformation would provide a direct instrument for solving the correspondence problem but since the assumption of the local surface planarity assumes the observation of a pixel group, plane homographic approach does not provide sufficient information for the active projection systems. However, it can be used with the passive systems where local planarity assumptions apply (e.g. in surface deformation measurements [12]).

### 3.2. Epipolar geometry

Epipolar approach defines the projection of image point  $p$  from one image plane to line  $l'$  in second the image plane, Figure 15. This is done by constructing a plane between image centers and the object point (shaded triangle in Figure 15), but camera relative orientation does not need to be known in advance. For a stereo-camera setup, the correspondence problem is satisfied for any pair of corresponding points ( $p \Leftrightarrow p'$ ) that satisfy [13,14]:

$$\mathbf{p}^T \mathbf{F} \mathbf{p}' = 0 \quad (5)$$

where fundamental matrix  $\mathbf{F}$  contains parameters describing system geometry and is valid for the entire image domain. The fundamental matrix can be derived

by using homographic transformations (4) of the point transferred via plane in space (Figure 14). The same homographical transformation is valid for the epipolar lines (Figure 15).

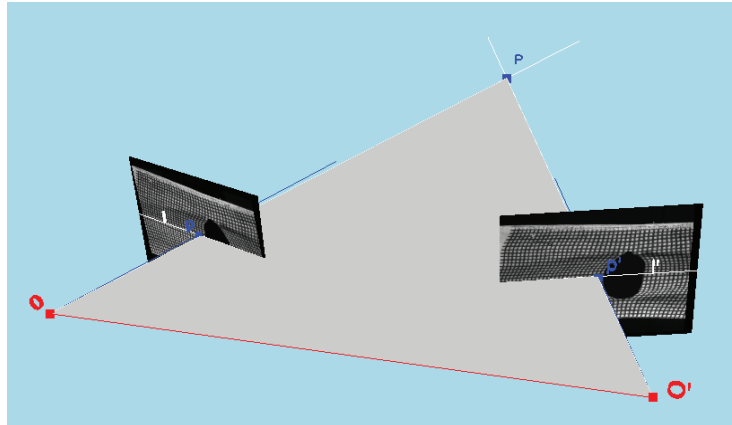


**Fig 15** Epipolar plane definition (shaded triangle)

**Sl. 15.** Definicija epipolarne ravnine (osjenčani trokut)

According to the epipolar principle, in the second camera, the epipole (point where line  $OO'$  intersect the image plane of the second camera) and point  $p'$  must lie on the epipolar line that can be defined as  $l' = e' \times p' = [e']_x p'$  [10]. This relation can be extended by the Eq. (4), as  $l' = [e']_x H p = F p$  where the relation between the fundamental matrix and homography is described as  $F = [e']_x H$ . Compared with piecewise unique solutions provided by homographic approach, the epipolar approach does not completely solve the correspondence problem. The advantage is that no assumptions regarding the geometric properties of the observed model are needed for the fundamental matrix computation (only that the geometry of both object and system is not changed during the image recording stage).

## 4. PASSIVE FULL-FIELD SYSTEMS

### 4.1. Digital image correlation based similarity

Marking measuring points with markers of a priori known geometry is not always possible, because either the measurement task requires full-field results or the marker application would block surface features because of marker finite size or shape. Instead of using specialized operators for searching image points with known shape, digital image correlation makes it possible to search for any

part of the reference image in the second image (which can be the same as the reference image), providing that the observed part has sufficiently different light intensity distribution than any other part of the second image. The observed part of the reference image is usually a square window (sometimes referred to as facet) whose size depends on the applied pattern and the curvature of the model surface. Similarity based operators try to minimize the error between chosen areas in both images, by searching for e.g. minimum of Sum of Absolute Distances or Sum of Squared Distances, or for the maximum in the Normalized Cross-Correlation functions.

$$\text{Sum of Absolute Distances (SAD)} \quad \sum_{i,j} |I_1(i, j) - I_2(x+i, y+j)| \quad (6)$$

$$\text{Sum of Squared Distances (SSD)} \quad \sum_{i,j} (I_1(i, j) - I_2(x+i, y+j))^2 \quad (7)$$

$$\text{Normalized Cross-Correlation (NCC)} \quad \frac{\sum_{i,j} I_1(i, j) I_2(x+i, y+j)}{\sqrt{\sum_{i,j} I_1^2(i, j) I_2^2(x+i, y+j)}} \quad (8)$$

Figure 16 brings an image whose intensity linearly changes from white on the left to black on the right. A square window measuring 9x9 pixels is chosen and its enlarged version shown in the lower right corner. SAD function is applied on the same image (when reference and target image are the same, this procedure is also known as autocorrelation) in order to find all the pixels with the chosen intensity distribution. The chosen window is a part of the reference image, so at least one accurate result should exist. Since the features of the reference image are repeated from top to bottom, the results should also follow this assumption, as seen in Figure 16 (right) where areas with the same intensity distribution are shown by overlapping squares, which now form a vertical line. In case of autocorrelation, the possibility of multiple solutions leads to the additional correspondence problems which can be avoided by using random pattern.

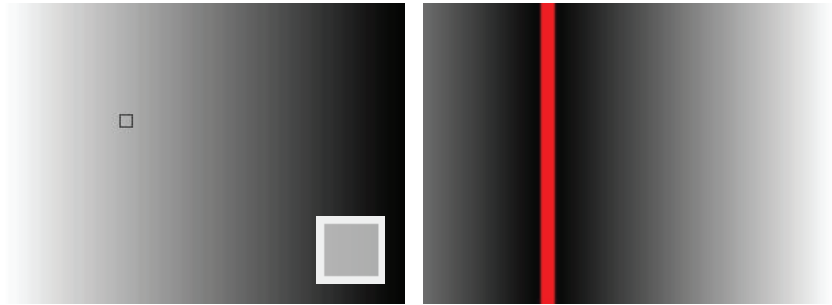


**Fig. 16** Autocorrelation example, original image (left), resulting image(right)

**Sl. 16.** Primjer autokorelacije, originalna slika (lijevo), rezultirajuća slika (desno)

In the resulting image (Figure 16, right) each pixel is colored by the normalized amount calculated by SAD function. The darkest areas show the most similar parts of the image, which are for SAD and SSD functions visualized as 3D graphs in Figure 17. Only the areas closest to the zero plane belong to the most similar areas of the image.

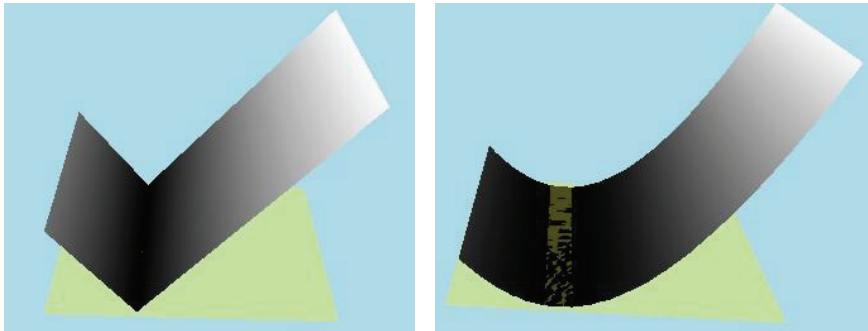


**Fig. 17** 3D view of SAD (left) and SSD (right) autocorrelation

**Sl. 17.** 3D vizualizacija SAD (lijevo) i SSD (desno) autokorelacije

The simplicity of the matching operator makes a measurable difference in the matching time because nowadays, digital images have several mega pixels. In our tests, SAD was the fastest of the three operators mentioned. Searching for similar image locations would be extremely computationally expensive if one were to use large facet sizes and try to compare each part of the reference image to each part of the second image. This procedure can be significantly simplified by utilizing the known camera geometry information. It is previously shown that for parallel camera setup, the stereo pair should lie along the horizontal pixel row of the referen-

ce image. For convergent camera setup instead of horizontal pixel rows, epipolar geometry or image rectification should be used. For a setup in which target image is different from the reference image (e.g. any stereo camera setup) it is possible that there is no point whose similarity measure is zero, since the same pattern will always look different in cameras displaced and rotated by any amount. Surface discontinuities can also occlude parts of the pattern, hiding the exact result. If one were to naively choose points with minimum difference, the resulting point cloud could be severely distorted. In order to avoid this problem, each stereo pair should be searched in a smaller disparity range, it is better to discard possibly accurate stereo pairs than to accept the completely wrong ones. There are implementations which search for neighboring stereo pairs by using a growing cluster around the manually selected starting point (e.g. Aramis by GOM).

#### 4.2. Passive stereo camera shape measurement

In case of passive shape measurement with two cameras, the reconstruction of shape can be performed by using only one image per camera. Figure 10 brings images that were recorded by two identical cameras in convergent setup, whose calibration parameters were unknown. Epipolar geometry can be reconstructed even if system parameters are unknown; in the first step, manual stereo pairs were found in both images (Figure 18). This step can be supported by using digital correlation functions, but due to the repeatable pattern, here it was not used. The fundamental matrix can be calculated by using singular value decomposition if 9 or more stereo pairs are known. There exist other algorithms that need fewer stereo pairs, but for the actual measurement purposes, having more stereo pairs is directly related to model stability, so here, 42 stereo pairs evenly distributed in both images were selected.

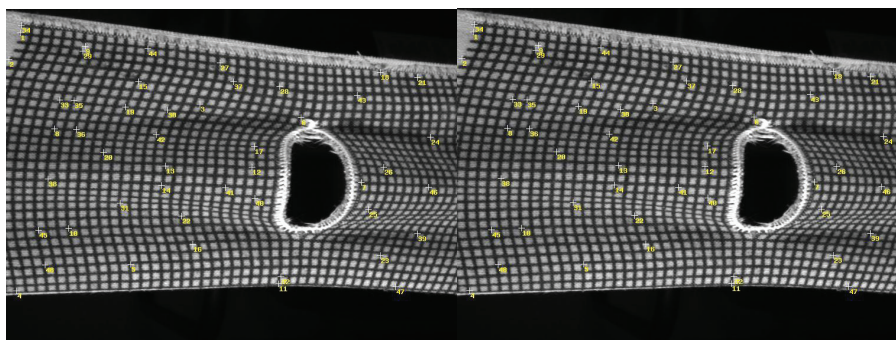


**Fig. 18** Stereo pair locations

**Sl. 18.** Prikaz odabranih stereo parova

After the calculation of the fundamental matrix  $F$ , epipolar lines were fitted through all the selected points in order to find outliers, Figure 19. Outliers can be filtered by statistical analysis. Once epipolar geometry is known one can search for stereo pairs as described in the previous sections; with constraint that each stereo pair has to be along the epipolar line in the second image.

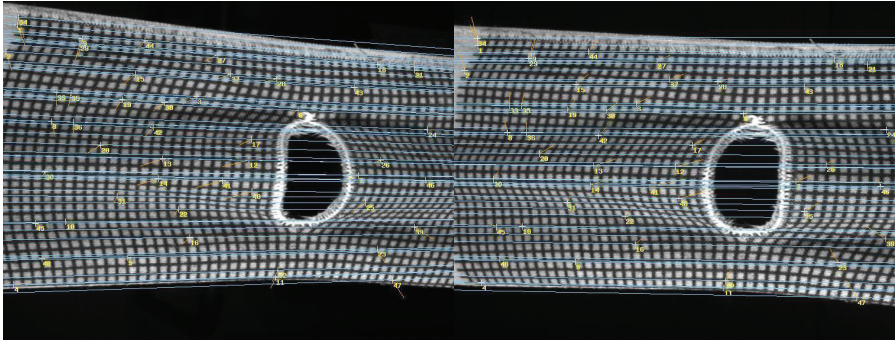


**Fig. 19** Epipolar lines  
**Sl. 19.** Epipolarne linije

If cameras were parallel, epipolar lines would also be parallel. The numerical camera rectification (Figure 20) is used here to reconstruct the view as would be seen from the parallel cameras. It is a numerical process that is based on the idea that epipoles (points of intersection of line connecting camera centers and image planes) for parallel camera setup have to be in infinity. For this numerical procedure, epipoles must not lie inside the visible part of the image plane, which can be controlled by camera angles.

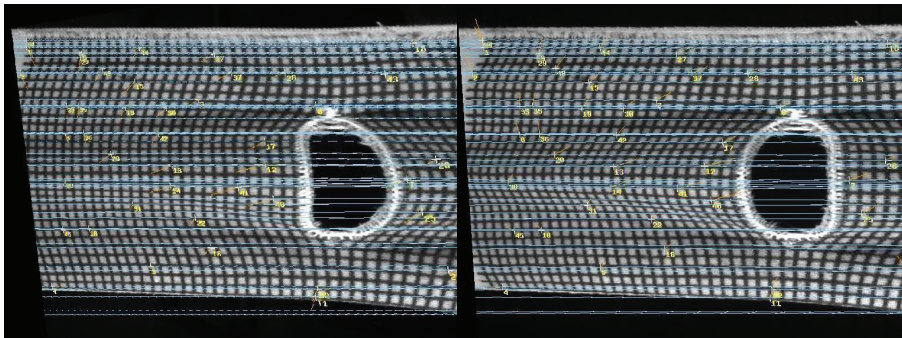


**Fig. 20** Numerically rectified images  
**Sl. 20.** Numerički ispravljene slike

After rectification, epipolar lines in Figure 20 are now horizontal and mutually parallel. The disparity map shown in Figure 21 has been obtained by using the left rectified image as reference and 15x15 pixel window with SAD operator. If camera parameters are known, the next step could be spatial point triangulation. For the visualization of geometry triangulation step is not necessary, because dark spots in the disparity map mark points away from the camera system, while white points mark those that are closer. Textured 3D visualization based on this mapping principle is shown in Figure 21 (right).

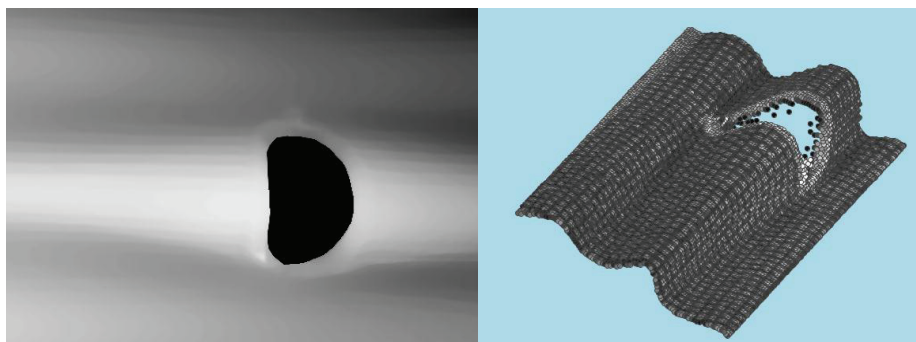


**Fig. 21** Disparity (left), 3D textured point cloud (right)

**Sl. 21.** Dispariteti (lijevo), 3D vizualizacija teksturiranog oblaka točaka (desno)

#### 4.3. Passive deformation measurement by the object grating method

The deformation measurements require one reference shape and at least one deformed shape, so that the procedure from the previous example can be used in full-field deformation measurements. If we assume that grating exactly follows the specimen deformation, grating optical features can be used for current stage shape reconstruction, as well as to find how and where the same point moved in time. For easier comparison of measuring points and for data reduction purposes, pictures for each stage are usually subdivided in facet field and compared in order to find each corresponding pair by using piecewise homography. For each stage, facets can be treated as stereo pair points if their average intensity for each stereo picture corresponds as follows:

$$g_1(x, y) = g_2(x_r, y_t) \quad (9)$$

where  $g_1$  and  $g_2$  represent the intensity of brightness for undeformed  $(x, y)$  and deformed  $(x_r, y_t)$  facets coordinates (Figure 22).

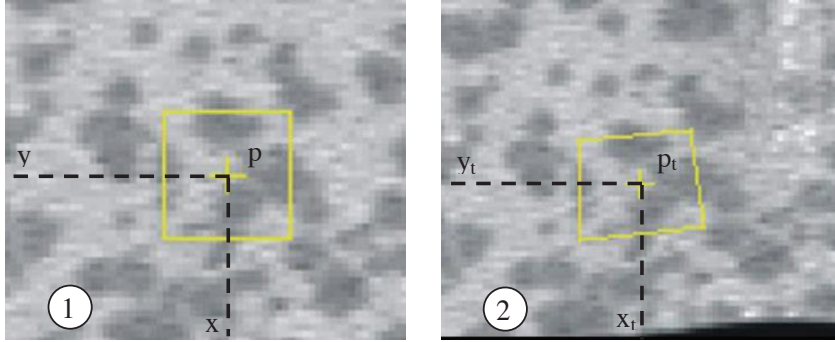


**Fig. 22** Distribution of 2D intensity in undeformed (1) and deformed (2) stage  
**Sl. 22.** Usporedba raspodjele intenziteta svjetloće u nedeformiranom (1) i deformiranom stanju (2)

The transformation of coordinates between stages by taking care of shift, rotation and deformation can be mathematically described using pseudo-affine transformation:

$$x_t = a_1 + a_2x + a_3y + a_4xy \quad (10)$$

$$y_t = a_5 + a_6x + a_7y + a_8xy \quad (11)$$

The left picture of the initial undeformed object is usually chosen as reference and subdivided into square windows of known sizes. Let us observe a single facet in unloaded stage located in the left image (Figure 23, Image 1), whose centre point  $p_1$  is selected at  $(x_{M1}, y_{M1})$ . The displacement transformation through images (according to Figure 23) can be expressed as follows:

$$\begin{pmatrix} x_{p1} \\ y_{p1} \end{pmatrix} = \begin{pmatrix} x_{M1} \\ y_{M1} \end{pmatrix} \quad (12)$$

$$\begin{pmatrix} x_{p2} \\ y_{p2} \end{pmatrix} = \begin{pmatrix} x_{p1} \\ y_{p1} \end{pmatrix} + \begin{pmatrix} u_2 \\ v_2 \end{pmatrix} \quad (13)$$

$$\begin{pmatrix} x_{p3} \\ y_{p3} \end{pmatrix} = \begin{pmatrix} x_{p1} \\ y_{p1} \end{pmatrix} + \begin{pmatrix} u_3 \\ v_3 \end{pmatrix} \quad (14)$$

$$\begin{pmatrix} x_{p4} \\ y_{p4} \end{pmatrix} = \begin{pmatrix} x_{p1} \\ y_{p1} \end{pmatrix} + \begin{pmatrix} u_4 \\ v_4 \end{pmatrix} \quad (15)$$

All points of the Figure  $x_{pi}, y_{pi}$  describe the same point on the object surface. With this information available, by using backward projection, object point coordinates can be calculated for every correct object point and for every stage. After the calculation of all three 2D displacements between the pictures of the deformed and reference state, 3D positions for every homological pair of points can be calculated (Figure 23).

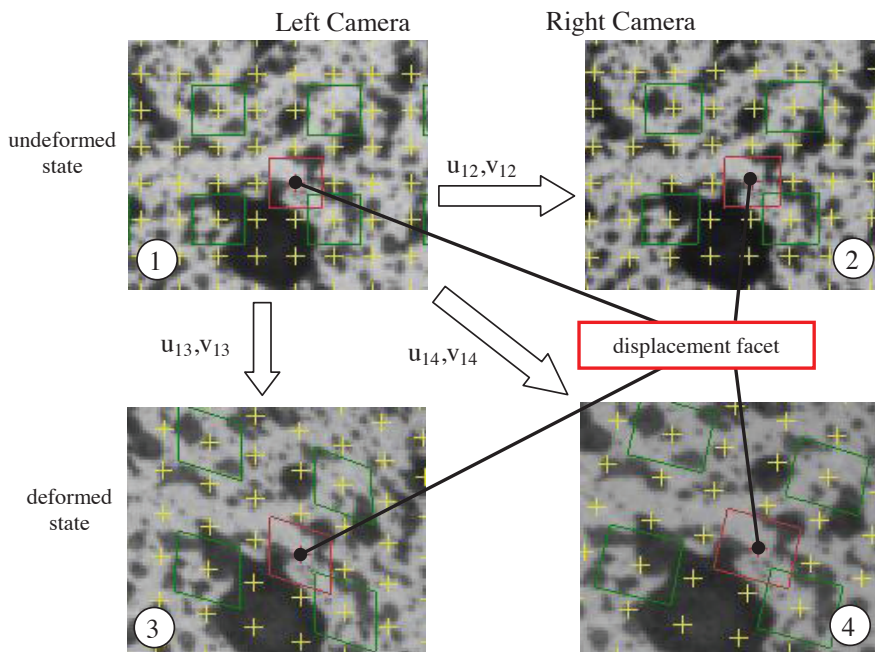


**Fig. 23** Determination of homological points  
**Sl. 23.** Određivanje homologijskih točaka

When 3D space coordinates for each measuring point are triangulated, the calculation of local strains follows numerically from the displacements fields [15-18]. Since 3D points lie on a surface of the specimen, the strain calculation is done by using small neighborhoods (usually 3x3 3D points). Best-fit surface is placed through these points, and outlier points are projected to it. Now, the strain analysis can be conducted in 2D space in a local coordinate system, by calculating strain tensor  $U$ , which relates to point positions between the deformed and undeformed states. The  $\epsilon_x$ ,  $\epsilon_y$  and  $\epsilon_{xy}$  values can be derived from the strain tensor  $U$ . To compute the major and minor principal strains for each facet, the eigenvalues are calculated from the strain tensor:

$$\varepsilon_{1,2} = 1 + \frac{\varepsilon_x + \varepsilon_y}{2} \pm \sqrt{\left(\frac{\varepsilon_x + \varepsilon_y}{2}\right)^2 - (\varepsilon_x \cdot \varepsilon_y - \varepsilon_x^2)} \quad (16)$$

Since the optical measurement technique does not register the change in thickness, the third principal strain  $\varepsilon_3$  can be calculated from the principal strains in the plane  $\varepsilon_1$  and  $\varepsilon_2$  only with the assumption that the volume is constant. In order to simplify the comparison of measured results with the standard uniaxial tensile tests according to [19] the effective von Mises strain can be introduced:

$$\varepsilon = \sqrt{\frac{2}{3}(\varepsilon_1^2 + \varepsilon_2^2 + \varepsilon_3^2)} \quad (17)$$

## 5. ACTIVE SYSTEMS

The development of the LCD projectors has enabled the extremely simple testing of various projection patterns. Patterns are used as an instrument to identify stereo pairs in each of the recorded images. It is common to all the projection patterns that they try to assign the unique numerical ID to each pixel (or pixel group). The position and numerical ID of a coded pixel will depend on the type of the projected pattern, but also on the analysis type, e.g. the coding by monochromatic intensity, color or by the projection of pattern of a known geometric shape. There are many coded light methods that can be summarized according to [20] in three categories: time coding, object coding and direct coding. The direct codification strategy projects pattern that is defined in such a way that a single projection is sufficient to code each image pixel, e.g. such color coding that each pixel or each line of pixels has a different color. It is extremely sensitive to the projector and camera linearity and to the change of the ambient lightning, since the projected sample definition can appear different in the recorded image because of the interaction with the local color of the surface of the observed object. It is not applicable in the sensitive measurement tasks due to the high amount of noise. The object coding of the measurement information is based on a projection of a single pattern that consists of structures, whose geometry and intensity distribution is known in advance. Single projection allows for it to be used in dynamical measurements. The object coded pattern can be of pseudo-random or exactly known shape, e.g. De Bruijn pattern or dashed parallel lines. The reconstruction of measurement information for a single pixel has to be conducted based on a group of neighboring pixels (often called facets), which is one of the

disadvantages of the object projection strategies, since it makes it difficult to scan surfaces that have big curvatures or edges and discontinuities. The advantage is in direct correspondence problem solving, since the pattern is often coded in such a way that a certain group of pixels will appear in image only once. The third group of codification strategies projects various pattern slides sequentially. Each of the pattern slides is defined in such a way that if analysis is conducted not in image domain like previous methods, but in the time domain, unique coding of each pixel can be obtained. This enables the analysis of each pixel separately to its neighbor, which contributes to method robustness. It avoids error propagation as it does not consider the neighboring pixels. High spatial resolution can be achieved by analyzing each pixel for itself. The pattern is generally very simple, usually consisting of binary coded parallel stripes. Due to the need for projecting series of slides in time, this method is not suitable for dynamical measurements.

### 5.1. Active stereo camera shape digitization system

The phase shifting model that belongs to time coding models will be here presented in detail. If we define the light intensity of a single pixel in the image plane  $I$  as:

$$I(x, y, t) = s(x, y, t) + a(x, y, t) \cos[\delta(x, y, t) + \varphi(x, y, t)] \quad (18)$$

where  $s(x,y,t)$  is mean overall intensity for some pixel,  $a(x,y,t)$  modulation,  $\delta(x,y,t)$  uniquely defined phase for each pixel and  $\varphi(x,y,t)$  additional reference phase. During the static object measurements unknown parameters  $s(x,y,t)$ ,  $a(x,y,t)$  and  $\delta(x,y,t)$  for all the image pixels actually do not depend on time, because changing time duration between projection of each slide does not change the intensity of each pixel for a given slide. These parameters can be considered as a function of the projector and the projected pattern, whose controlled displacement  $\varphi(x,y,t)$  is changed. In order to find those three unknowns, we need to record a minimum of three images, but to minimize noise, it is common to use the over-defined system with four or more projected patterns. In a case of four phase images,  $\delta(x,y)$  can be expressed as:

$$\delta(x, y) = \arctan \frac{I_2 - I_4}{-I_1 + I_3} \quad (19)$$

Phase shifting principle will be explained by simulating projection on a flat plane and recorded by a left camera of the two-camera system. Four projections of the same pattern, each shifted by  $\pi/2$  are illustrated in Figure 24 (left).

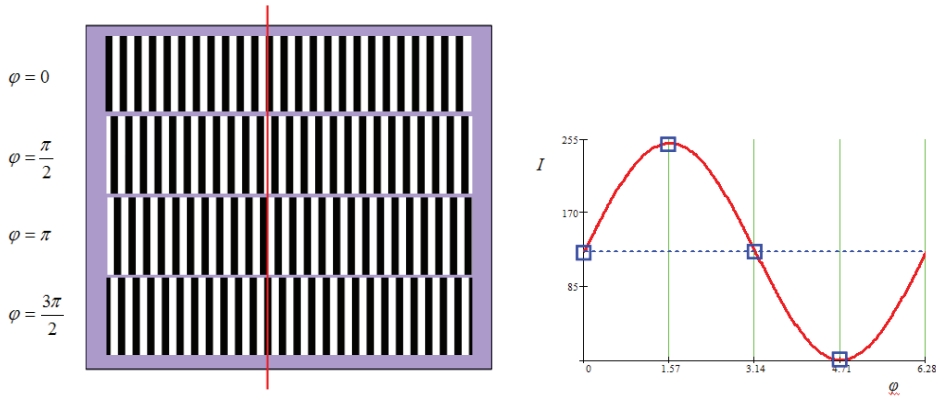


**Fig. 24** Phase shifting principle

**Sl. 24.** Princip vremenskog faznog pomaka

The projected pattern consists of parallel black fringes followed by equally wide white ones. Edges between fringes are in this example sharp, but for the actual measurements phase noise will be lower if the grating is sinusoidal in horizontal direction. If we assume that the pattern is projected parallel to pixels in the camera, and that in this example, the phase shift is introduced to the right, then vertically stacked projected stripe samples show how the intensity of each pixel changes in time. Intensity variation for a given pixel in time is defined by a vertical cross-section of Figure 24 (left). A given pixel in the first projection observed in the left image is located on the edge of the projected lines. In second projection shifted by  $\pi/2$  that pixel is completely white, followed by another projected edge and a completely dark stripe during the last projection. If 8-bit camera were used, the completely white pixel had the intensity of 255 and the completely dark pixel 0. In our example, the pixel in the the first slide will have the intensity about 128, in the second slide shifted by  $\pi/2$  the intensity will be 255, then 128 and finally 0, which is illustrated by squares in Figure 24 (right). If we fit equation 18 through these points, the resultant position of the entire sinusoidal curve is a partial phase for a given pixel, calculated by Eq. (19). If measurements were carefully conducted, and both camera and projector were linear, then mean value and modulation should be unified over the entire image. Figure 24 (right) should look the same for a neighboring pixel, slightly shifted in phase. The shift direction depends on the direction of the projected pattern shift; the amount depends on how far the observed pixel is from the referent one. Due to the repeating nature of the projected pattern, pixels with the same repeating codes will exist on the pixels separated by one black and one dark fringe. This will result in the saw-tooth like partial-

phase image (Figure 25, left) with the apparent repeating pattern (taken from the actual measurement). The repeating effect disables the unique identification of a certain phase in the right image as the partial phase value repeats multiple times across the horizontal row of pixels, as shown in Figure 25 (right).

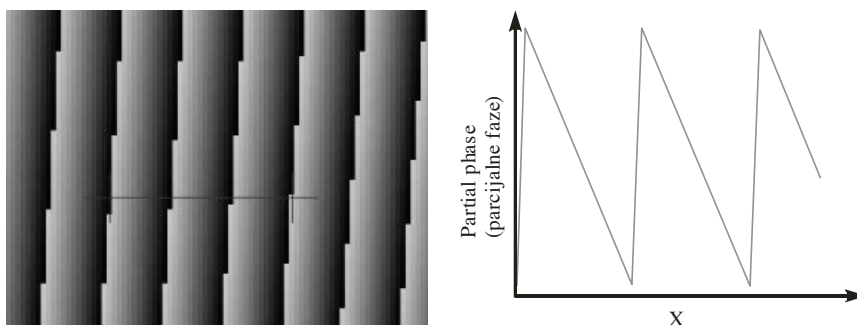


**Fig. 25** Detail of partial phase distribution  
**Sl. 25.** Detalj raspodjele parcijalnih faza

In order to solve this additional correspondence problem, for the absolute phase calculation, the binary stripe projection coded by the Gray code principle has been used. The method is based on the consecutive thickening of the projected lines. By the careful projection of six patterns [20], the area, where each “tooth” of the partial phase is defined, is coded by a combination of light and dark fields. It results in a stair-like Gray code image (Figure 26, left), where the width of each stair corresponds to the width of the phase tooth. The height of each stair is a multiple of  $2\pi$ , Figure 26 (right).

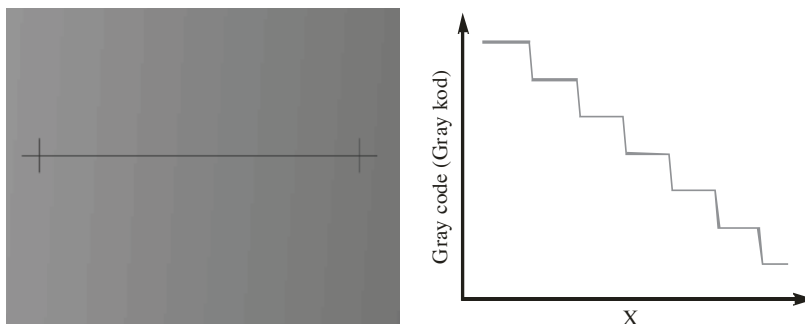


**Fig. 26** Detail of Gray code distribution  
**Sl. 26.** Detalj raspodjele Gray koda

The reconstruction of absolute phases in both images (Figure 27) is reduced to the sequential summation of partial phases (saw-tooth like image) with the Gray code stair-like image. It has to be done for each pixel, in each image separately. The absolute phase associated with each pixel is reconstructed independently from its neighbors, thus reducing the error in locating the position of neighboring areas. The stripe projection results in the absolute phase image where phases are repeated in the vertical direction (in the ideal setup); in real setups they are almost vertical, as seen in Figures 25 and 26. The correspondence problem is not entirely solved, since the same absolute phase is still repeated in the vertical direction (in Figure 27 marked with vertical lines). Systems consisting of two cameras and a projector thus need to exploit their geometric over-determination. A stereo pair is defined as a cross-section of the line consisting of the observed absolute phase and the epipolar line in each image, as illustrated in Figure 27.

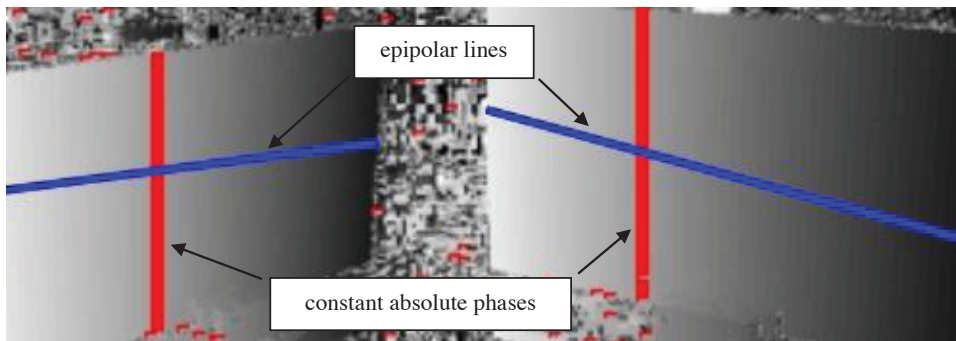


**Fig. 27** Absolute vertical-phase distribution for a planar specimen, shown in both cameras  
**Sl. 27.** Raspodjela apsolutnih vertikalnih faza na planarnom objektu, u obje kamere

## 5.2. Active multi camera system

Commercial systems that use two cameras in a convergent setup find stereo pairs as explained in section 5.1. This procedure might require initial system calibration, which can be avoided by the introduction of the additional perpendicular projection pattern. The digitization can be conducted by projecting two mutually perpendicular patterns, consisting of combination of phase shift and Gray code [21,22], as illustrated in Figure 28. In that way, each correctly illuminated pixel in cameras carries information of both the horizontal and vertical phases. Finding a stereo pair is now a problem of searching for the pixel with equivalent codes in the image domain, without the need of epipolar geometry

or homography. The search procedure has to be conducted in two phase images per camera. It is simplified by knowing that projected patterns were perpendicular and the direction of phase increase for each pattern is known. The analysis of search algorithms will be conducted on the assumption that perpendicular patterns were projected on a flat surface, while horizontal pixels match in the cameras used. Camera pixels have integer coordinates, thus the initial analysis will only use integer values. After the calculation of horizontal and vertical phases from the phase and Gray code images, one pixel is selected in the reference camera (usually the left one), so its horizontal and vertical phases are known. It is followed by searching the picture of vertical phases from the second camera, until the column with the exact vertical phase is found. Under the perpendicularity condition, the horizontal phase has to be positioned somewhere along the column from the vertical absolute phase image. This procedure is repeated for all correctly coded and digitized pixels.

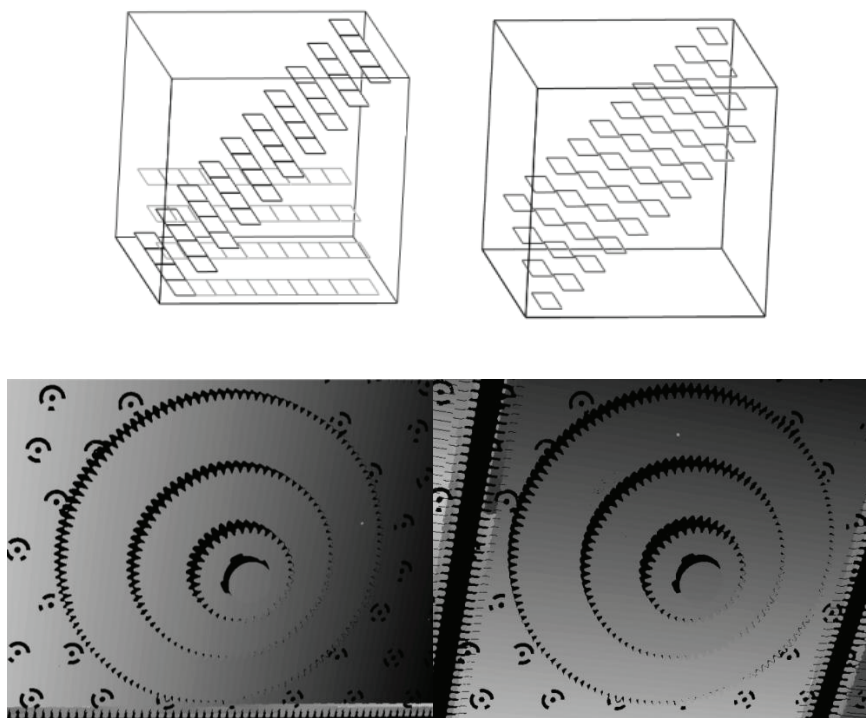


**Fig. 28** Illustration of the double coding (upper left); the sum of the horizontal and vertical phase images (upper right), absolute phases in double coded camera 1 (lower left).  
**Sl. 28.** Ilustracija dvostrukog kodiranja (gore lijevo), zbroj horizontalnih i vertikalnih faznih slika (gore desno), apsolutne faze u dvostruko kodiranoj kameri 1 (dolje)

This method can be extended so that instead of looking for integer pixel, one looks for the pixel placed one row up and one column left from the selected pixel. It is now similar to object methods, since a small facet consisting of four pixels is used. It allows a bilinear interpolation of the non integer position of the target pixel. This is practical in the case of real cameras, since they provide images that are a discretization of the actual surface. Due to the need for a certain angle between the cameras (usually somewhere in the range of  $20^\circ$ - $30^\circ$ ) projected patterns are not always mutually perpendicular and parallel to camera pixel rows and columns. This approach has the advantage of reducing the noise in the reconstructed cloud, but it uses information from the neighboring pixels, thus converging towards object methods. The two-way projection has reduced the need for the epipolar geometry and assigns two different phases to each image, but this method still cannot be directly compared to the absolute object methods because it does not assign one unique ID to each pixel. It can be clearly seen if we add both phases into a unique phase, as illustrated in Figure 28 (upper right). Now the same ID (represented by height) repeats under a  $45^\circ$  angle, and additional control mechanism is needed to find the correct stereo pair. In two-camera systems that use pattern projection in only vertical direction, the Gray code has contributed to the correspondence problem solving by unwrapping partial phase images. The resulting absolute phase image is an approximately monotonous plane. The Gray code has not contributed to the accuracy of the overall method. Its contribution is only in giving the exact direction for phase unwrapping. Absolute phases obtained by vertical projection can be used analogous to the Gray code in two-camera systems [23], while absolute phases projected in horizontal direction were used for recovering absolute phases. The principle will be explained on the 8-bit image sample consisting of four lines, each 10 pixels wide. Let the intensity of the first pixel in a row be zero and of the last 255. Due to graph clarity, the phase in the horizontal projection increases to the right. If a single pixel is chosen in vertical absolute phase image obtained by projecting on the flat plane (under the condition that pixels are parallel to horizontal phases), that pixel will have a phase that is repeated in the vertical phase image along the selected row. That row will be used as the initial line. Relative movements during the pattern projecting are not allowed; let us now read each pixel from the horizontal phase image. This leaves us with a discrete phase distribution that looks like a small staircase line. If the projected image consisted of only that line, the correspondence problem would be automatically solved because each pixel would contain its own unique ID defined by the horizontal phase. This procedure is repeated for a next row in the vertical phase image for a pixel with the first larger vertical phase value. The second line of horizontal phases is obtained. It is the neighboring line from the

previous stage, Figure 29 (left). Since those two lines consist of equal or similar horizontal phase values, but with integer difference in the vertical phases, the correspondence problem is still not solved. It would be absolutely solved only if each pixel that both lines consist of had a unique ID that would repeat in our 20 pixels only once. Next step is to increase all vertical phases from the second line for some constant value. In case images were recorded by 8-bit cameras with 256 light levels and phase images were projected with 64 light and dark stripes, the largest horizontal or vertical phase expectable for a row of pixels is  $256 \cdot 64 = 16384$ , in that case, we would have to increase each row of vertical phases by  $16384 + 1$ . That step is increased by one, so that the first pixel from second row would not interfere with the last pixel from the first row. It is a minimal step needed to differentiate both lines, while in our simplified example, the sufficient step would be  $10 + 1$ . Using any other step higher than minimal would also result in the absolute phase image. Now, each pixel in the two observed lines of the horizontal phase images is coded by a unique code, which proves the absolute indexing possibility of a perpendicular projection technique. The advantage of this approach is the possibility of using any other projection technique that can provide two perpendicular phase images (e.g. direct perpendicular projection of color coded lines or heterodyne pattern). If we repeat this procedure for the remaining pixels, the resulting absolute phases in our example are shown in Figure 29 (right). Compared to Figure 28 (upper right), each unique code is now repeated only once, and the stereo pair searching can now be done in a single image per camera. This procedure has to be conducted for all cameras involved. Each image can be considered as the indexed set, which associates two image coordinates to each absolute ID. The stereo pair reconstruction now can be conducted simply by converting

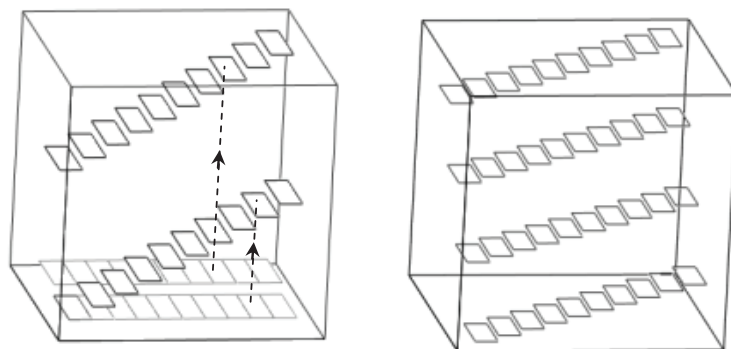


**Fig. 29** Absolute phases for (left) two rows of pixels, (right) whole model  
**Sl. 29.** *Apsolutne faze za (lijevo) dva reda piksela, (desno) cijeli model*

image into the single pixel line, by adding each horizontal phase row one after the other. This approach reduces the two-dimensional searching problem to a one-dimensional problem. Searching for stereo pairs in a one-dimensional array is faster than searching through horizontal and vertical phase images, especially as the next target index is most likely the next neighbor to the previous index.

The solution is straightforward if the problem is observed as the intersection of two indexed sets keeping two image coordinates for each absolute ID. Finding stereo pairs is now reduced to reading the same index in all of the cameras. This approach avoids the need for a reference camera, as well as for the usage of searching and sorting algorithms. The correspondence problem solving procedure is now reduced to the pixel-by-pixel array manipulation.

## 6. CONCLUSIONS

In the optical measurement field, regardless of the number of used cameras and the way the measuring point is defined, in order to extract the measurement data, it is necessary to solve the correspondence problem in the fastest and most efficient way. Due to a large variety of internal and external influencing factors, it is not always clear which the best possible way to do it is, unless one understands how the correspondence problem progresses from single via stereo- to the multiple-camera systems. This motivated us for writing a critical review of passive and active single and stereo shape and deformation measurement systems, where we presented the important parts of their mathematical models and how they behave in the real world measurements. Special focus was on the stereo and multi-camera active systems where we presented a new method for stereo pair indexing. By using a modified projection approach, we showed that it is possible to eliminate the need for the epipolar principle from the correspondence problem solving. With the new indexing method, each pixel can be used as a separate measuring point, since it is indexed with two independent absolute phases. Searching for stereo pairs is also reduced from the two-dimensional image domain to a one-dimensional array where the next stereo pair is most likely the nearest neighbor to the observed one. Our next efforts are to incorporate this knowledge into the multi-camera passive deformation measurement systems.

## References

- [1] N. Drvar, S. Jecić, P. Knežević, V. Vedran, The experimental model for biomechanical research of midface, 4th Youth Symposium on Experimental Solid Mechanics, Italy 2005. 23-24
- [2] J. Kodvanj, A. Bakić, B. Ljubenkov, M. Gomerčić, N. Drvar, The Use of Photogrammetry in Shape and Dimensional Control in Shipbuilding, Brodogradnja 2005, 48-53
- [3] N. Drvar, Razvoj optičkog mjernog sustava za neposredno mjerenje deformacija epruveta na univerzalnim kidalicama, seminarski rad, FSB Zagreb, 2003
- [4] B. Jahne, Digital Image Processing, 5th ed., Springer, 2002.
- [5] A. Gruen, T. S. Huang, Calibration and Orientation of Cameras in Computer Vision, Springer Series in Information Sciences, Germany, 2001.
- [6] A.F. Habib, M. Morgan, Y.-R. Lee, Bundle Adjustment with Self-Calibration Using Straight Lines, The Photogrammetric Record 17 (100), 635–650, 2002.
- [7] J. Salvi, X. Armangue, J. Batlle, A comparative review of camera calibrating methods with accuracy evaluation, Pattern Recognition 35, 1617-1635, 2002.
- [8] S. Jecić, N. Drvar, 3D shape measurement influencing factors, MATEST 2004, KBR - Kompetentnost i sigurnost, Zagreb 2004. 109-116
- [9] S. Jecić, N. Drvar, The assessment of structured light and laser scanning methods in 3D shape measurements, 4th International Congress of Croatian Society of Mechanics, Zagreb 2003. 237-244
- [10] R. I. Hartley, A. Zisserman, Multiple View Geometry in Computer Vision, Cambridge University Press, 2004.
- [11] A. Agarwal, C. V. Jawahar, and P. J. Narayanan: A survey of planar homography estimation techniques, IIIT Technical Report IIIT/TR/2005/12, 2005
- [12] N. Gubelj, D. Semenski, N. Drvar, J. Predan, D. Kozak, M. Oblak, Object grating method application in strain determination on CTOD tests, Strain, May 2006, Vol. 42, Iss. 2, 81-87.
- [13] J-A. Beraldin et al., *Active 3D Sensing*, Modelli E Metodi per lo studio e la conservazione dell'architettura storica, NRC 44159, pp 22-46, 2000.
- [14] D. Forsyth, J. Ponce, *Computer Vision: A Modern Approach*, Prentice Hall, 2003.
- [15] M. Gomerčić, N. Drvar, A Novel Videoextensometer for Strain Measurement on Tensile Testing Machines, In: Proceedings of the 18th Danubia-Adria-Symposium on Experimental Methods in Solid Mechanics, Steyr, 2001, 47-48
- [16] C. Steger, Evaluation of subpixel line and edge detection precision and accuracy, International Archives of Photogrammetry and Remote Sensing, Vol. XXXII (1998) Part 3/I, 256-264

- [17] N. Drvar, D. Semenski, J. Skoko, Integration of the object grating method into numerical elastoplastic material modeling, *Proceedings of the 19th Danubia-Adria Symposium on Experimental Methods in Solid Mechanics*, 2002, 84-85
- [18] N. Drvar, The aspects of tensile testing machine stiffness on measured results, *Extended summaries of TC15-youth imeko symposium on experimental solid mechanics*, Bologna, 2002, 35-36
- [19] ARAMIS user manual v6, 2007
- [20] J. Salvi, J. Pages, J. Batlle, Pattern Codification Strategies in Structured Light Systems, *Pattern Recognition* 37(4), pp. 827-849, April 2004.
- [21] M. Gomerčić, *Doprinos automatskoj obradi optičkog efekta u eksperimentalnoj analizi naprezanja*, doktorska disertacija, FSB Zagreb, 1999.
- [22] M. Gomerčić, S. Jecić, A New Self-Calibrating Optical Method For 3d-Shape Measurement, *17th Symposium Danubia-Adria on Experimental Methods in Solid Mechanics*, Prag 2000. 113-116
- [23] N. Drvar, *Optički postupak digitalizacije oblika projiciranjem kodiranog svjetla*, doktorska disertacija, FSB Zagreb, 2007.

## Problem jednoznačnosti kod optičkih metoda mjerjenja oblika i deformacija

### Sažetak

Problem lociranja i jednoznačnog prepoznavanja jedne te iste točke na više uzastopno ili istovremeno snimljenih slika tijekom optičkih mjerjenja oblika ili deformacija poznat je pod pojmom jednoznačnosti. Javlja se kada postoji potreba za praćenjem neke optičke karakteristike u svim snimljenim slikama, neovisno o broju korištenih kamera i broju snimljenih slika. U ovom su radu kritički uspoređena rješenja problema jednoznačnosti kod pasivnih i aktivnih sustava s jednom kamerom, stereo sustava s dvije kamere i vlastito razvijenog sustava s više kamera. Posebno je za aktivni sustav s više kamera razvijena apsolutna metoda za jednoznačno indeksiranje stereoparova. Korištenjem modificiranog projekcijskog pristupa pokazano je kako je iz postupka za rješavanje problema jednoznačnosti moguće eliminirati potrebu primjene epipolarnog principa. Nova metoda indeksiranja omogućava da svaki piksel u kameri postaje zasebna mjerna točka, jer je indeksirana s dvije međusobno neovisne apsolutne faze. Ovom modifikacijom je pretraga cijele dvodimenzij-ske domene slike svedena na pretragu jednodimenzijskog reda kod kojega je sljedeći traženi stereopar susjed trenutno promatranoj točki.

*Ključne riječi:* optička mjerjenja, oblik, deformacije, sustav sa više kamera, problem jednoznačnosti, metoda faznog pomaka, Gray kod, digitalna korelacija slike

Akademik **Stjepan Jecić**  
University of Zagreb  
Faculty of Mechanical Engineering  
and Naval Architecture  
Ivana Lučića 5, 10000 Zagreb  
E-mail: stjepan.jecic@fsb.hr

Dr. sc. **Nenad Drvar**  
University of Zagreb  
Faculty of Mechanical Engineering  
and Naval Architecture  
Ivana Lučića 5, 10000 Zagreb  
E-mail: nenad.drvar@fsb.hr